MULTI-MATERIAL TWO-TEMPERATURE MODEL FOR SIMULATION OF ULTRA-SHORT LASER ABLATION

Mikhail E. Povarnitsyn[*1, 2], Tatiana E. Itina[1]
[1]Laboratory of Lasers, Plasmas and Photonic Processing (LP3, UMR 6182 CNRS), Faculté des Sciences de Luminy, Case 917, 13288, Marseille, France
Konstantin V. Khishchenko[2], Pavel R. Levashov[2]
[2] Institute for High Energy Densities RAS, Izhorskaya 13/19, Moscow, 125412, Russia

Abstract

We investigate the interaction of 100 fs laser pulses with metal targets at moderate intensities (10^{12} to 5×10^{13} W/cm^2). To take into account effects of laser energy absorption and relaxation we develop a multi-material two-temperature model based on a combination of different approaches. The backbone of the numerical model is a high-order multi-material Godunov method in a purely Eulerian form. This formulation includes an interface-tracking algorithm and treats spallation at high strain rates and negative pressures. The model consistently describes the hydrodynamic motion of a two-temperature plasma and accounts for laser energy absorption, electron-phonon/ions coupling and electron heat conductivity. In particular, phase transitions are accurately taken into account by means of a wide-range two-temperature multi-phase equation of state in a tabular form. The dynamics of the phase transitions and the evolution of the heat-affected zone are modeled and analyzed. We have found that a careful treatment of the transport coefficients, as well as consideration of phase transitions is of a great importance in obtaining reliable numerical results. Calculation results are furthermore compared for two metals with different electron-phonon coupling parameters (Au and Al). We have found that the main part of ablated material results from fragmentation of melted phase caused by tensile stresses. A homogeneous nucleation mechanism alone does not explain experimentally observed ablation depth.

PACS: 61.80.Az; 79.20.Ds; 64.70.Dv; 64.70.Fx

[*] Corresponding author: tel: +33 (0) 491 829 285; fax: +33 (0) 491 829 289, E_mail: povarnitsyn@lp3.univ-mrs.fr

Keywords: Laser interactions; Laser ablation; Laser melting; Heat transfer; Laser-induced spallation

1. Introduction

Theoretical investigations of the ultrashort laser-matter interaction by using the well-known two-temperature model (TTM) have long history [1]. In metals, conduction band electrons absorb laser energy and then transmit it inside the target due to their thermal conductivity. At the same time, the lattice is heated in electron-ion collisions. This simple formulation does not, however, guarantee quantitative agreement with experiments. In fact, numerical solution turned out to be sensitive to a number of governing parameters, such as electron-phonon collisions rate, thermal conductivity coefficient, optical absorption depth, spall strength, which in turn may be functions of temperature, density etc. That is why recent investigations were focused on more accurate definition of these coefficients [2, 3]. Molecular dynamics (MD) studies [4, 5] showed details of the laser-matter interaction processes on atomic level. These calculations, for instance, helped in better understanding of the internal mechanisms responsible for the processes of voids growth and coalescence. Spall strength at high strain rates and thermal softening are also investigated by experimental methods [6]. In addition, several models of fragmentation were also proposed [7, 8]. Nevertheless there is still no complete understanding of the mechanisms of voids formation in liquid and solid phases at high strain rates and short times for different materials. In this paper we present the results of the simulation of laser melting and ablation of both aluminum and gold targets irradiated by 100 fs laser pulses. The computational model used for the description of laser-metal interaction is discussed. Considerably different electron-phonon relaxation time for Al and Au results in different pictures of evolution of basic parameters for these metals.

2. Computational model

We describe the processes of laser-matter interaction by using classical continuous hydrodynamics. Our numerical model for tracking multiple substances is based on the extension of a high-order multi-material approach [9] using the two-temperature ideology similar to that of Ref 1. For simplicity, one-dimensional compressible equations are written for two-temperature multi-material hydrodynamics in the Euler's form with laser energy absorption source, electron heat conductivity and electron-phonon energy exchange terms as follows:

$$\frac{\partial f^{\alpha}}{\partial t} + \frac{\partial (f^{\alpha} u)}{\partial x} = \frac{f^{\alpha} \overline{K}_S}{K_S^{\alpha}} \frac{\partial u}{\partial x}, \tag{1}$$

$$\frac{\partial (f^{\alpha} \rho^{\alpha})}{\partial t} + \frac{\partial (f^{\alpha} \rho^{\alpha} u)}{\partial x} = 0, \tag{2}$$

$$\frac{\partial (\overline{\rho} u)}{\partial t} + \frac{\partial (\overline{\rho} u^2 + \overline{P})}{\partial x} = 0, \tag{3}$$

$$\frac{\partial}{\partial t}\left[f^{\alpha} \rho^{\alpha} \left(E_e^{\alpha} + \frac{u^2}{2} \right) \right] + \frac{\partial}{\partial x}\left[f^{\alpha} \rho^{\alpha} u \left(E_e^{\alpha} + \frac{u^2}{2} \right) \right] + \frac{f^{\alpha} \rho^{\alpha}}{\overline{\rho}} u \frac{\partial \overline{P}}{\partial x} =$$

$$- \overline{P}_e \frac{f^{\alpha} \overline{K}_S}{K_S^{\alpha}} \frac{\partial u}{\partial x} + Q_L^{\alpha} - f^{\alpha} Q_{ei}^{\alpha} + \frac{f^{\alpha} \rho^{\alpha} C_e^{\alpha}}{\overline{\rho} \overline{C}_e} \frac{\partial}{\partial x}\left(\overline{\kappa}_e \frac{\partial \overline{T}_e}{\partial x} \right), \tag{4}$$

$$\frac{\partial (f^{\alpha} \rho^{\alpha} E_i^{\alpha})}{\partial t} + \frac{\partial (f^{\alpha} \rho^{\alpha} E_i^{\alpha} u)}{\partial x} = - \overline{P}_i \frac{f^{\alpha} \overline{K}_S}{K_S^{\alpha}} \frac{\partial u}{\partial x} + f^{\alpha} Q_{ei}^{\alpha}, \tag{5}$$

Here, f^{α}, K_S^{α}, C_e^{α} and ρ^{α} are the volume fraction, isentropic bulk modulus, specific heat capacity of electrons and the density of the α component, respectively; u is the hydrodynamic velocity (common for electrons and heavy particles), $\overline{P} = \overline{P}_e + \overline{P}_i$ is the sum of electronic and ionic pressures, $\overline{\kappa}_e$ is the "effective" electron heat conductivity, $\overline{T}_e$ is the mean temperature of electrons, E_e^{α} and E_i^{α} are the specific internal energies of electrons and ions, Q_L^{α} and Q_{ei}^{α} are the laser energy absorption source and electron-ion energy exchange term, respectively.

Volume fractions are subjected to the condition $\sum_{\alpha} f^{\alpha} = 1$, the average density in a multi-material cell is $\overline{\rho} = \sum_{\alpha} f^{\alpha} \rho^{\alpha}$ and effective heat capacity of electrons is $\overline{C_e} = \frac{1}{\overline{\rho}} \sum_{\alpha} f^{\alpha} \rho^{\alpha} C_e^{\alpha}$. An effective isentropic bulk modulus and thermal conductivity of the "mixture" are expressed by means of the individual properties of the components as follows: $1/\overline{K_S} = \sum_{\alpha} f^{\alpha} / K_S^{\alpha}$ and $\overline{\rho}\overline{C_e} / \overline{\kappa_e} = \sum_{\alpha} \left(f^{\alpha} \rho^{\alpha} C_e^{\alpha} / \kappa_e^{\alpha} \right)$, where κ_e^{α} is the electron heat conductivity of the α component. Note, that at the chosen time and space scales of the present calculations, the temperature equilibration processes occur faster than the pressure equilibration ones. For this reason we use splitting of the equation (4) and describe separately the process of electron heat conductivity with effective (equilibrated at each time step) temperature $\overline{T_e}$ using implicit numerical scheme. The model of the heat conductivity of electrons is taken from [10]. The electron-phonon energy exchange term, the reflectivity coefficient and the optical penetration depth are derived from the wide-range frequency of electron-phonon collisions [11] using the Drude's theory.

The used Eulerian formulation of basic equations is more advantageous than the Lagrangian one because of the simple spatial splitting. On the other hand, the Euler's formulation requires a special procedure for interfaces reconstruction [12].

A Gaussian temporal profile is used to simulate the laser energy deposition in the form $I(x,t) = I_L (1-R) \exp[-\ln(16)(t-t_0)^2 / \tau_L^2] \exp[-x/\lambda_{opt}]$, where I_L is the laser pulse intensity, R is the reflectivity coefficient, τ_L is the full width at half maximum (FWHM) of the pulse and λ_{opt} is the optical penetration depth. The connection between the laser fluence F and intensity I_L for Gaussian time profile in one direction is $F = I_L \sqrt{\pi / \ln(16)} \tau_L$. Then, the absorbed

energy is calculated as $Q_L = I(x,t)/\lambda_{opt}$, and the redistribution between several materials is performed proportionally to the individual mass fractions $Q_L^\alpha = \frac{f^\alpha \rho^\alpha}{\overline{\rho}} Q_L$.

Finally, a special treatment was used for the photomechanical failure of the material. In fact, there is still a lack of information about this effect on the microscopic level. Even extremely high tensile strengths obtained in our simulations do not satisfy the criteria of fragmentation proposed in [7, 8] because of the short duration time (tens of picoseconds), whereas the fragmentation (homogeneous nucleation) of liquid phase was previously observed both in ablation experiments and in recent MD simulations. To tackle this problem we use a criterion of fragmentation for liquid phase of gold obtained in the MD simulations [4], where the minimum possible negative pressure is -2 GPa. We set an instantaneous damage of liquid phase when the pressure drops below this value, by introducing the void into computational cell and by relaxing pressure to zero in this cell.

For completeness of our model, we construct a semiempirical equation of state (EOS) for each material with separated components of electrons and lattice (heavy particles) using ideas described in [13]. More details about the equations of state will be presented elsewhere.

3. Results and discussion

We focus on the problem of phase transitions and spallation mechanism. The simulation results show that the ablated material may consist both of gas and liquid phases. During the laser pulse irradiation the temperature of electrons rapidly grows within the skin layer and then the lattice temperature increases due to electron-phonon collisions. Depending on the laser pulse fluence in our simulations melting and even ablation of the lattice is possible. The energy expenditure or calorification during the phase transitions is taken into account by means of the EOS with separated phase states (see [14, 15] for details).

Figure 1 shows the calculated evolution of main parameters of the target of Au irradiated by 5 J/cm^2 (4.7×10^{13} W/cm^2) and τ_L = 100 fs. One can see in the Figure, that at a delay of approximately 5 ps the shock wave (SW) is formed nearby the target surface. Figure 1(c) demonstrates that the SW goes deep into the target and it is followed by a rarefaction wave (RW). The RW leads to a negative tensile stress and causes spallation of the liquid phase by the time 40 ps (Fig. 1(a)). After that, the gaps between individual droplets increase. At the same time, as it can be seen from Fig. 1(b), the disintegration of the substance severs the heat conduction mechanism and prevents the temperature equilibration between the separated material chunks. The time-space distribution of the phase states is presented in Figure 1(d). The Figure demonstrates that the initial speed of the melting front is about 6 km/s and the speed of shock wave is 4 km/s. By the time delay of 20 ps, the shock wave overcomes the melting front. Because of the low electron-phonon energy exchange rate both the lattice temperature and pressure increase slowly, so that the hydrodynamic rarefaction of the target is not too strong. That is why the velocity of chunks (clusters) is sufficiently small. Furthermore, the calculated ablation depth is found to be mainly governed by the melting region size. In all considered cases, the gas fraction (evaporated material) represents only several percents of the total mass of the ablated material.

The EOS used in the calculations contains information about phase states. Therefore, we can follow the trajectories in the phase plane as a function of different radiation conditions. After an isochoric heating of the material, relaxation begins and some trajectories can cross the liquid-gas equilibrium boundary. Then, the substance may go through metastable states of liquid and gas (see Fig. 1(d)). The similar thermodynamic trajectories were observed and analyzed in the MD simulations [5] for regions of the target where homogeneous nucleation occurred.

In contrast to gold, aluminum has a much shorter electron-phonon relaxation time. As a result, the lattice heating of aluminum is localized in a narrower zone. Fast energy exchange causes both steeper lattice pressure profile and more intensive rarefaction of the target material. The first cluster (chunk) appears at a delay of 20 ps and travels at 1.4 km/s, whereas the latest one arises at 50 ps and moves away with a small velocity (see Fig. 2(a)). Small fractions fly ahead of the liquid clusters and consist of the liquid-gas metastable phase. Elastic oscillations are obviously visible for thick clusters (Fig. 2(d)). Similar oscillations were also observed in the previous MD simulations [16]. A comparison with experimental data was performed mainly for the ablation depth. A good agreement between simulation and experiment shows the importance of taking into account different processes of laser energy absorption by metallic targets.

4. Summary

We have developed a self-consistent physical model that is used for the simulation of main processes occurring in metallic targets irradiated by moderate subpicosecond laser pulses. Melting front propagation and phase transitions during the heating and spread of the target material is considered using multi-phase EOS in tabular form with separated components of electrons and heavy particles. The transport properties of the laser-irradiated materials are calculated by using the wide-range model of electron-phonon collision frequency. The fragmentation of the liquid phase due to a strong tensile stress and high strain rate leads to the production of chunks and clusters. These clusters fly away from the target. Negative pressures that appear in the solid phase during the propagation of the rarefaction wave can be strong enough but their duration is typically too short to cause spallation of the material.

Acknowledgment

One of the authors, MEP gratefully acknowledges the financial support from the CNRS, France. We are thankful to the IDRIS and the CINES of CNRS, France for the computer support.

References

[1] S.I. Anisimov, B.L. Kapeliovich, and T.L. Perel'man, Zh. Eksp. Teor. Fiz., **31**, 776 (1974), [Sov. Phys. JEPT, **39**, 375 (1974)].

[2] J.P. Colombier, P. Combis, F. Bonneau, R. Le Harzic, and E. Audouard, Phys. Rev. B, **71**, 165406 (2005).

[3] C. Schäfer, H.M. Urbassek, and L.V. Zhigilei, Phys. Rev. B, **66**, 066415 (2002).

[4] D.S. Ivanov, L.V. Zhigilei, Phys. Rev. B, **68**, 064114 (2003).

[5] D. Perez, L. J. Lewis, Phys. Rev. B, **67**, 184102 (2003).

[6] G.I. Kanel, S.V. Rasorenov, A.A. Bogatch, A.V. Utkin, V.E. Fortov, and D.E. Grady, J. Appl. Phys., **79**(11), 8310-8317 (1996).

[7] D. E. Grady, J. Mech. Phys. Solids, **36**(3), 353-384 (1988).

[8] G.I. Kanel, S.V. Rasorenov, and V.E. Fortov, J. Appl. Mech. Tech. Phys., **25**(5), 701-711 (1984).

[9] G. H. Miller and E.G. Puckett, J. Comput. Phys., **128**(1), 134 (1996).

[10] S.I. Anisimov and B. Rethfeld, Proc. SPIE Int. Soc. Opt. Eng. (USA) 3093, p.192-203 (2002).

[11] K. Eidmann, J. Meyer-ter-Vehn, and T. Schlegel, and S. Hüller, Phys. Rev. E, **62**(1), 1202-1214 (2000).

[12] J. E. Pilliod, E. G. Puckett, J. Comput. Phys., **199,** 465-502 (2004).

[13] Ya. B. Zel'dovich, and Yu.P. Raizer, Academic, New York, 1966, Chap. 1.

[14] K.V. Khishchenko, S.I. Tkachenko, P.R. Levashov, I.V. Lomonosov, and V.S. Vorob'ev, Int. J. Thermophys., **23**, 1359-136 (2002).

[15] V.I. Oreshkin, R.B. Baksht, N.A. Ratakhin, A.V. Shishlov, K.V. Khishchenko, P.R. Levashov, and I.I. Beilis, Phys. Plasmas, **11**, 4771-4776 (2004).

[16] R. Knochenmuss, and L.V. Zhigilei, J. Phys. Chem. B, **109**, 22947-22957 (2005).

Figure captions

Figure 1.

Calculated properties of a gold target as a function of time and space for laser pulse with τ_L = 100 fs, λ=800nm, and F = 5.0 J/cm^2. (a) Density, g/cm^3. (b) Lattice temperature, 10^3 K. (c) Pressure, GPa. (d) Phase states: metastable gas (1), metastable liquid-gas mixture (2), metastable liquid (3), metastable melting (4), metastable solid (5), solid (6), melting (7) and liquid (8).

Figure 2.

The same as in Figure 1, but for aluminum. Here, (9) is the stable gas on the diagram of phase states (d).

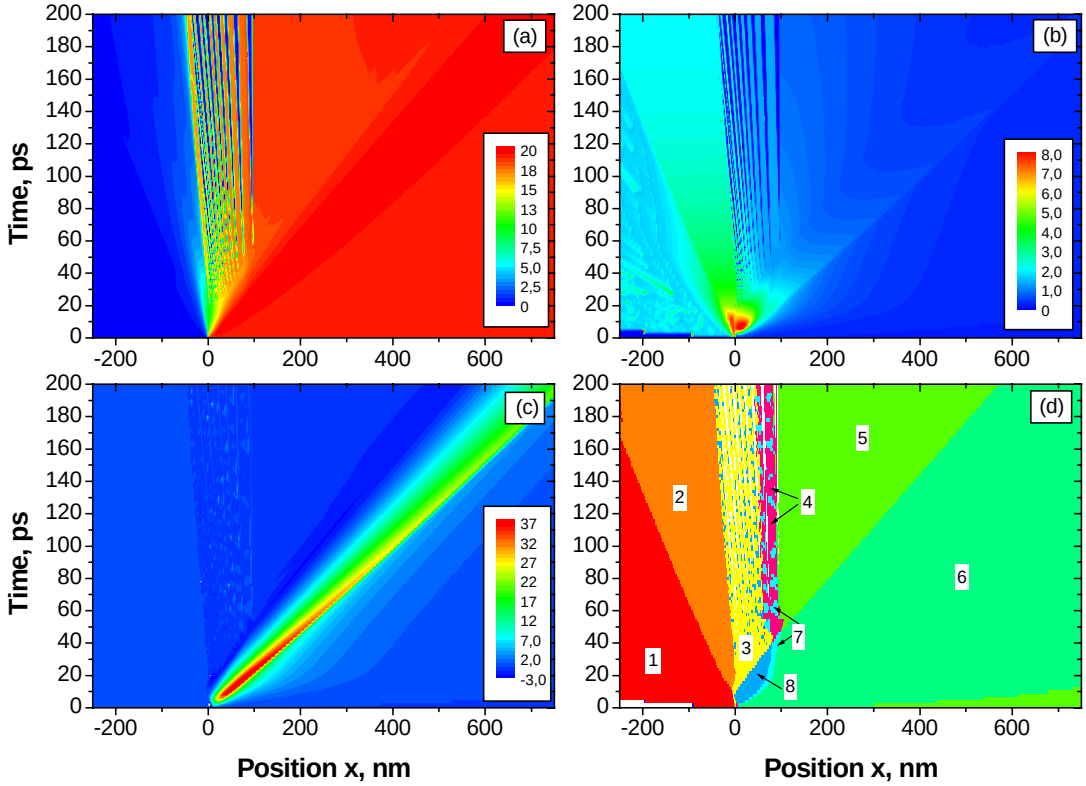

Figure 1

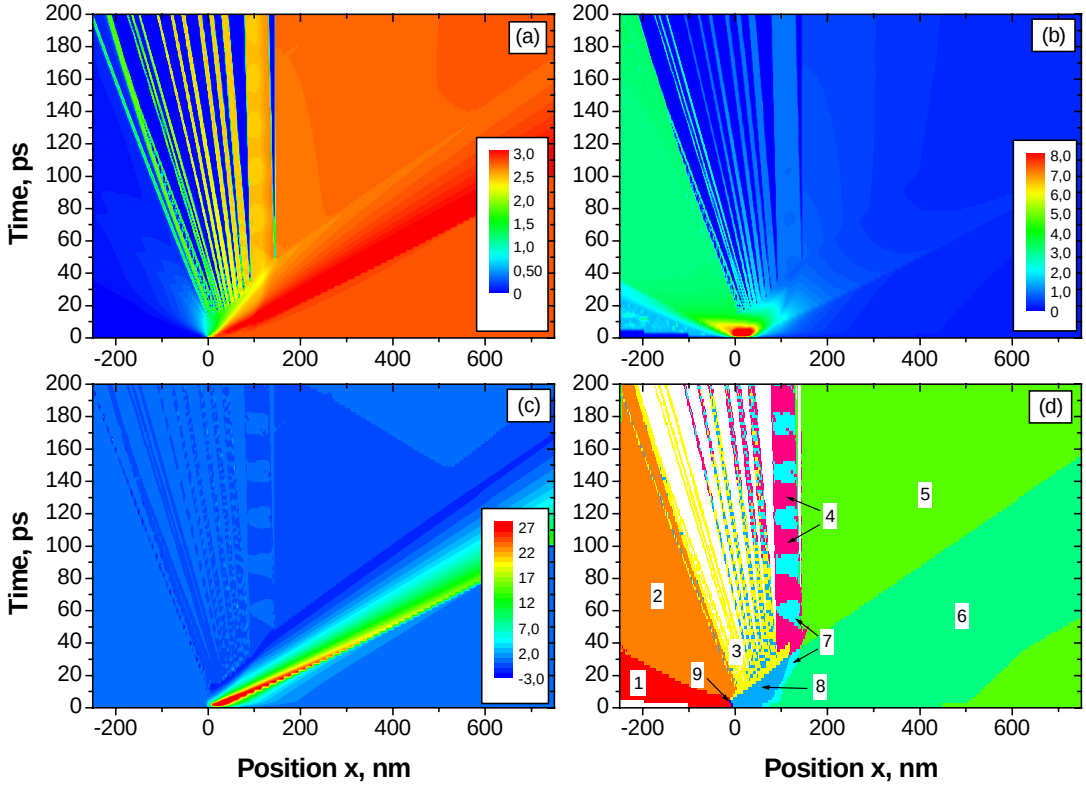
(a)
(b)
(c)
(d)
Time, ps
Position x, nm
3,0
2,5
2,0
1,5
1,0
0,50
0
8,0
7,0
6,0
5,0
4,0
3,0
2,0
1,0
0
27
22
17
12
7,0
2,0
-3,0
1
2
3
4
5
6
7
8
9

Figure 2